Bull. Mater. Sci., Vol. 35, No. 3, June 2012, pp. 399–404. © Indian Academy of Sciences.

Effect of nano-CeO_2 on microstructure properties of TiC/TiN+nTi(CN) reinforced composite coating

LI JIANING, CHEN CHUANZHONG* and ZHANG CUIFANG

Key Laboratory for Liquid-Solid Structural Evolution and Processing of Materials (Ministry of Education), Department of Materials Science, Shandong University, Jinan 250061, Shandong, China

MS received 8 April 2011; revised 1 August 2011

Abstract. **TiC/TiN+TiCN reinforced composite coatings were fabricated on Ti–6Al–4V alloy by laser cladding, which improved surface performance of the substrate. Nano-CeO_2 was able to suppress crystallization and growth of the crystals in the laser-cladded coating to a certain extent. With the addition of proper content of nano-CeO_2, this coating exhibited fine microstructure. In this study, the Al_3Ti+TiC/TiN+nano-CeO_2 laser-cladded coatings were studied by means of X-ray diffraction and scanning electron microscope. The X-ray diffraction results indicated that the Al_3Ti+TiC/TiN+nano-CeO_2 laser-cladded coating consisted of Ti_3Al, TiC, TiN, $Ti_2Al_{20}Ce$, $TiC_{0.3}N_{0.7}$, $Ce(CN)_3$ and CeO_2, this phase constituent was beneficial to increase the microhardness and wear resistance of Ti–6Al–6V alloy.**

Keywords. **Rare-earth compounds; surface modification; laser cladding; microstructure; X-ray diffraction; intermetallic compounds.**

1. Introduction

Laser cladding is an advanced surface modification technology that uses a high power laser beam to form a composite coating with specific quality and low dilution that is metallurgically bonded to the substrate, which can greatly improve wear resistance of the substrate (Dutta Majumdar *et al* 2000, 2009; Wang *et al* 2010). TiC and TiN showed excellent properties of low density, wear resistance, etc (Wang *et al* 2007). During the laser cladding process, TiC can react with TiN leading to formation of titanium carbonitride (TiCN), which showed superior mechanical properties, such as low friction, high hardness (2500–3000 HV), high melting point (3050°C) and enhanced wear resistance (Forn *et al* 2001).

Laser cladding of the Al_3Ti+TiC/TiN pre-placed powders on the Ti–6Al–4V alloy formed the TiC/TiN+TiCN reinforced Al_3Ti/Ti_3Al matrix composite coating, which can greatly improve surface performance of the substrate. It was known that titanium aluminides have a lot of good performance, such as low density, high specific strength, elastic modulus, wear resistance and better mechanical behaviour with temperature (Hisashi *et al* 2008). In addition, cerium as rare earth elements (RE), has been applied successfully in many fields. An area of current interest is the modification of RE to surface engineering. An earlier study (Baligidad and Khaple 2009) indicated that Ce was able to refine microstructure of laser-cladded coatings, and also improved strength and ductility of the coatings. Furthermore, in the field of surface engineering, nano-materials have been found in the literature on laser cladding and laser surface alloy, which have a lot of excellent properties, such as strong acoustic, electric, magnetic and thermodynamic characteristics because of their quantum size and surface effect (Zeng *et al* 2002). Moreover, if amorphous layer is desired, then CeO_2 should dissolve, depress the fusion/eutectic temperature, stabilize the melt and retain glassy layer after laser cladding. Throughout the experiment, it was found that the CeO_2 particles were easily reunited because of the surface effect. The agglomeration of CeO_2 particles was generally located on the grain boundaries, which were able to suppress the crystallization and growth of the TiN/TiC precipitates to a certain extent.

Our present work is aimed at the investigation of the microstructure and wear resistance of the Al_3Ti+TiC/TiN laser-cladded coatings with or without CeO_2.

2. Experimental

Cross-flow CO_2 laser cladding equipment was used in this experiment. The main components of laser cladding equipment are: CO_2 laser device (maximum power, 1·5 kW and it may be adjusted continuously), the optical system, the working table and operation system. It should be mentioned that too high power can burn out a portion of the pre-placed powders, which can greatly influence quality of the coatings. Reversely, the laser power decided the inter-diffusion of substrate material to the cladded material, and the laser surface alloying cannot occur completely with too low power. Hence, in this research, the power was in the range of 850 ~ 1000 W.

The materials used in this experiment were Ti–6Al–4V alloy and powders of Al_3Ti (≥99·5% purity, 50 ~ 150 μm), TiC (≥99·5% purity, 50 ~ 150 μm), TiN (≥99·5% purity, 50 ~ 150 μm) and CeO_2 (≥99·5% purity, 10 ~ 200 nm) for

*Author for correspondence (czchen@sdu.edu.cn)

Table 1. Parameters and materials of laser-cladding process in the experiment.

Number	Substrate material	Powder compositions (wt%)	Laser power (W)	Scanning speed (mm s^{-1})	Spot diameter (mm)
Sample 1	Ti–6Al–4V alloy	Al_3Ti–20TiC–35TiN	850 ~ 1000	2 ~ 6	4
Sample 2		Al_3Ti–20TiC–20TiN			
Sample 3		Al_3Ti–20TiC–20TiN–1·5CeO_2			

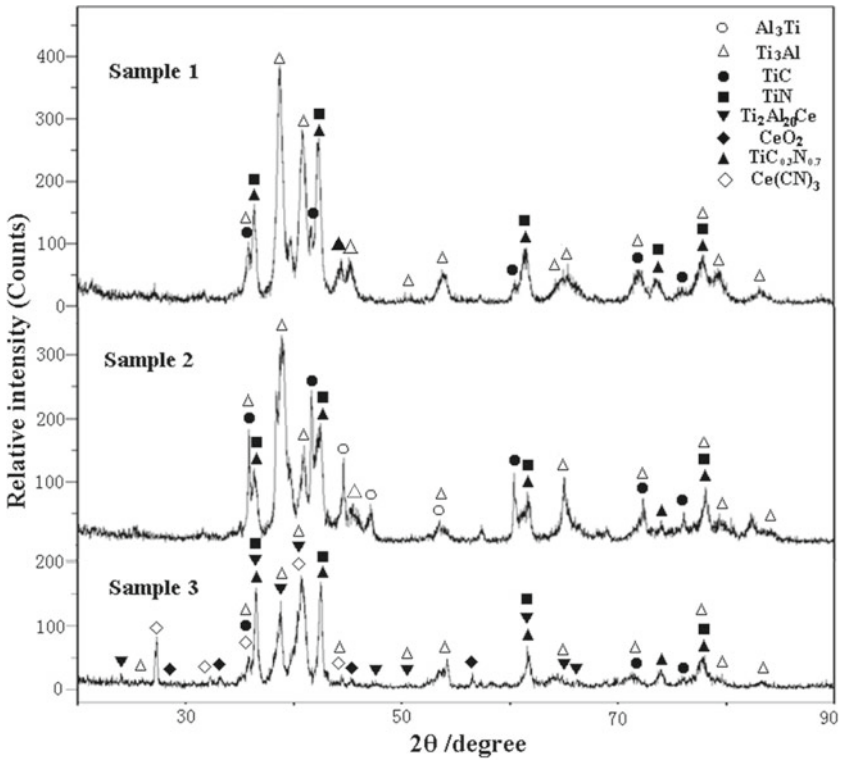

Figure 1. X-ray diffraction diagrams of coatings in samples 1, 2 and 3.

laser cladding. The size of the samples of Ti–6Al–4V alloy was 10 × 10 × 10 mm. The thickness of pre-placed layer was 0·6 ~ 0·8 mm, three-track lap coating was formed on samples, and the lap rate was ~30%. To protect the molten pool from oxidation, during the laser cladding process, the coating surface was prevented by inert gas (Ar) with a flow rate of 30 l/min. The parameters and materials of this experiment are shown in table 1.

According to the report of Zhao *et al* (2000), it was known that too excessive rare-earth oxide can form many inclusions, which would markedly reduce wear resistance of the composite coatings. On the other hand, we also found that an obvious improvement in wear resistance of Al_3Ti+TiC/TiN laser-cladded coating was not achieved with too little CeO_2 content. Thus, 1·5 wt% nano-CeO_2 was used in this study.

MM200 disc wear tester was used to test wear resistance of the laser-cladded coatings, the rotational speed of the wear tester was 400 r/min, and load was 5 kg. The wear mass loss increased proportionally with prolonged friction time. The honing wheel was made of quenching and tempering steels (W18Cr4V).

The samples were polished and etched in a hydrofluoric acid + nitric acid aqueous solution. The volume ratio of hydrofluoric acid, nitric acid and aqueous solution was 1:2:3 which revealed growth morphology of the compounds in the laser-cladded coatings. DMAX/2500PCX X-ray diffraction (XRD) was used to determine the phase constituents of these composite coatings. The microstructure morphologies of the composite coatings were analysed by means of QUANTA200 scanning electron microscope (SEM). The element distributions of the composite coatings were measured using JXA-880R electron probe micro-analyser (EPMA). HV-1000 microsclerometer was used to test the microhardness distribution of the composite coatings.

3. Results and analysis

3.1 *XRD analysis*

The overlap of XRD patterns of the composite coating in samples 1, 2 and 3 illustrated a significant phase evolution after laser cladding. As shown in figure 1, it was seen that

the phase area of the coating surface in sample 1 consisted of Ti_3Al, TiC, TiN and $TiC_{0.3}N_{0.7}$, and the matrix of the coating mainly consisted of Ti_3Al.

It was noticed that $TiC_{0.3}N_{0.7}$ was produced in the coating due to the reaction between a portion of TiC and TiN, the reaction was described as follows:

$$0{\cdot}3TiC + 0{\cdot}7\ TiN \rightarrow TiC_{0.3}N_{0.7}. \quad (1)$$

Moreover, it was also found that only Ti_3Al diffraction peak was present in XRD pattern of sample 1. It should be considered that during the cladding process, a portion of TiN dissolved to deliver amount of Ti into the molten pool, so a Ti-rich molten pool was produced. Therefore, Al_3Ti can further react with Ti in molten pool leading to production of Ti_3Al.

XRD result of the coating in sample 2 indicated that with the decrease of TiN content, the TiC diffraction peak increased significantly. It was known that the melting point of TiC (3150°C) was higher than that of TiN (2950°C), so it can be deduced that during the freezing time, TiC precipitated earlier than TiN. Thus, TiC was the nucleus in the precipitation, and TiN precipitated around it. It was reasonable that with the decrease of mass fraction of TiN pre-place powder, the content of TiN precipitates around TiC also decreased, thus resulting in the enhancement of TiC diffraction. On the other hand, according to (1), with the decrease of TiN, the production of $TiC_{0.3}N_{0.7}$ consumed less TiC leading to high TiC diffraction peak and low diffraction peak of $TiC_{0.3}N_{0.7}$.

With the addition of nano-CeO_2, there were Ti_3Al, TiC, TiN, $Ti_2Al_{20}Ce$, $TiC_{0.3}N_{0.7}$, $Ce(CN)_3$ and CeO_2 in the coating of sample 3. $Ti_2Al_{20}Ce$ was produced due to the reaction between Al_3Ti and nano-CeO_2 particles. It should be considered that the production of $Ti_2Al_{20}Ce$ consumed a large amount of Al in the molten pool. Hence, with the decrease of Al, a Ti-rich molten pool was achieved leading to the disappearance of Al_3Ti. According to the report of Tian *et al* (2006), during the cladding process, a portion of CeO_2 was decomposed as follows:

$$CeO_2 \rightarrow Ce + O_2\uparrow. \quad (2)$$

Then, Ce was able to further react with TiC/TiC leading to the formation of $Ce(CN)_3$ and Ti particles. Though the experiment was processed under the protection of the inert gas, the carbide/nitride were not stable at higher temperatures under oxygen, and a portion of them went to oxide that can also lead to off stoichiometry and decrease of TiN/TiC. However, due to the short solidification time and surface treatment to the samples, this influence on the laser-cladded coatings was not serious.

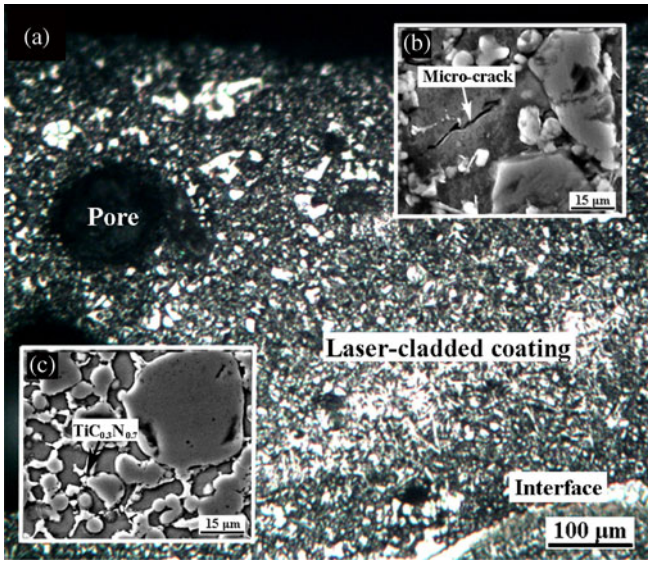

Figure 2. Microstructure of coating in sample 1: (**a**) cross-sectional view with low magnification, (**b**) unmelted TiC/TiN block and micro-crack and (**c**) $TiC_{0.3}N_{0.7}$.

3.2 *Microstructure*

3.2a *Microstructure of Al_3Ti+TiC/TiN laser-cladded coatings*: Figure 2 showed the microstructure of the overview cross-section of the laser-cladded coating in sample 1. It was noted that there were pores and cracks in this coating. In fact, the dilution rate of the substrate to the coating decreased with

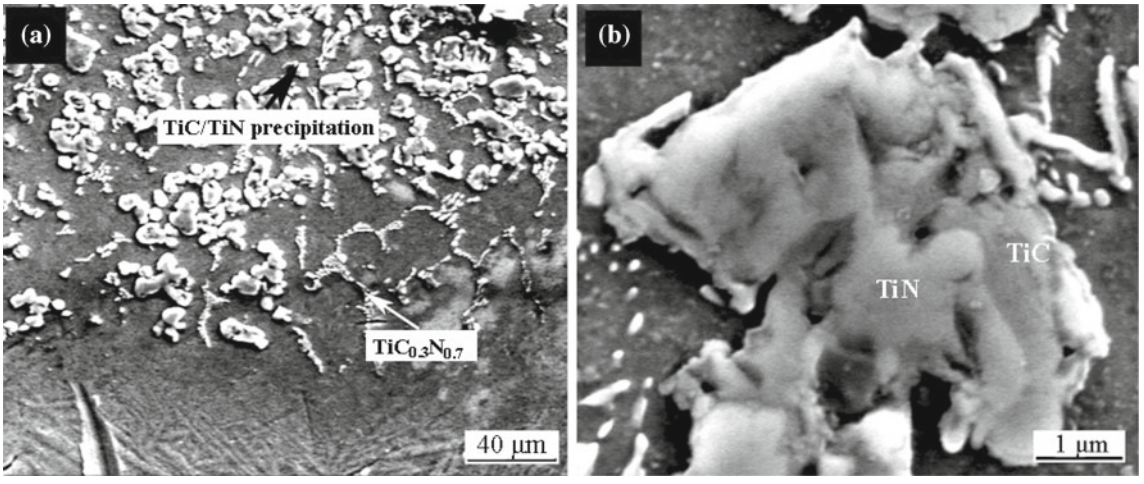

Figure 3. SEM micrographs of coating in sample 2: (**a**) interface and (**b**) TiC/TiN precipitates.

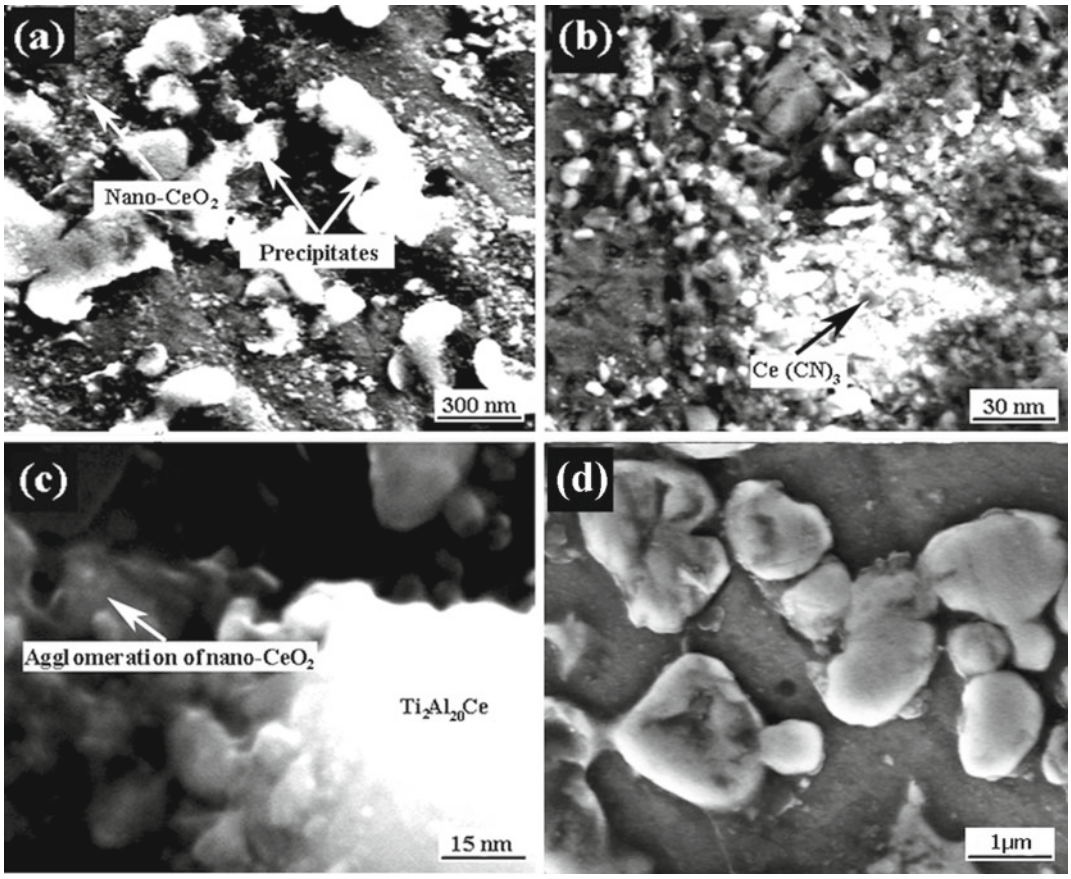

Figure 4. SEM micrographs of composite coating in sample 3: (**a**) clad zone, (**b**) nano-CeO_2 and $Ce(CN)_3$, (**c**) agglomeration of nano-CeO_2 and (**d**) $TiC_{0.3}N_{0.7}$.

the increase of the TiC/TiN content, which led to decreased energy of the laser beam that was transmitted onto the Ti–6Al–4V substrate. Therefore, freezing time of the molten pool was short, and the steam did not have enough time to escape, leading to the formation of the pores.

On the other hand, due to the high TiC/TiN content, the thermal stress of the laser-cladded coating in sample 1 was greater than the materials yield strength limit, thus resulting in the production of micro-crack (see figure 2b). Combining the XRD result, amount of $TiC_{0.3}N_{0.7}$ was produced in the coating (see figure 2c), which was a solid solution of FCC TiN and FCC TiC incorporating the advantages and characteristics of both TiN and TiC (Ertuerk *et al* 1991).

As shown in figure 3(a), it was noted that there was a metallurgical combination between the coating in sample 2 and Ti–6Al–4V alloy substrate. During the cladding process, the $TiC_{0.3}N_{0.7}$, TiC and TiN particles acted as dendrite nuclei, which were dispersed in the molten pool. Furthermore, the larger depth of laser melting pool and the rapid convection by a high energy density led to distribution of the $TiC_{0.3}N_{0.7}$ precipitates to a deeper depth, because the density of $TiC_{0.3}N_{0.7}$ was larger than those of TiC/TiN (Yang *et al* 2010). As shown in figure 3(b), it was noted that the bulk-shape precipitates were present in the clad zone. Nevertheless, its surface was not smooth, and there were protuberant block-shape precipitations adjacent to it. As mentioned earlier, protuberant precipitations consisted of TiN, and the bulk-shape precipitation below it was TiC.

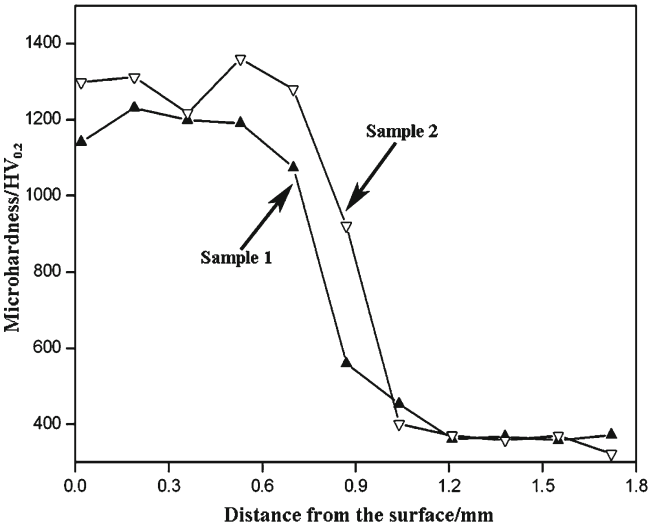

Figure 5. Microhardness distributions of coatings in samples 1 and 2.

3.2b *Microstructure of Al_3Ti+TiC/TiN+nano-CeO_2 laser-cladded coating*: Figure 4(a) shows that fine TiC/TiN precipitates were dispersed in the coating. Furthermore, there were also amount of nano-CeO_2 particles dispersed in the coating, and uniform distribution of nano-CeO_2 particles was advantageous to improve the hardness and wear resistance of the coatings. On the other hand, as mentioned earlier, a portion of CeO_2 was decomposed into Ce and O_2 during the cladding process. It was also observed earlier that Ce was able to refine the microstructure coatings and reduced the secondary dendrite spacing (Li *et al* 2008). Thus, the composite coating in sample 3 showed finer microstructure than that of the coating in sample 2. Moreover, combining the XRD results, the $Ce(CN)_3$ metal cyanide was produced in this coating (see figure 4b). Lai *et al* (1993) reported that the production of the metal cyanide can further enhance the microhardness of the composite coating.

In addition, once the molten layer formed, the dispersoids dissolved partially or fully and hence, nano-CeO_2 can neither remain CeO_2 nor nanometric in size. However, the energy distribution of the laser beam was uneven. Thus, a portion of the nano-CeO_2 particles in the edge of facula were able to retain the nanometric size, which diffused into every location of the molten pool due to their high diffusion coefficient (Zhang *et al* 2008). Then, these nano-CeO_2 particles become nucleation site during the solidification process, which was beneficial in refining the microstructure of the coating. Combining the XRD result, the enwrapped-like $Ti_2Al_{20}Ce$ phase was formed in the coating of sample 3 and then grew up via incomplete peritectic reaction (Zhao *et al* 2010). In addition, it was noted that agglomeration of the nano-CeO_2 particles was present in the coating (see figure 4c), this was indicated that nano-CeO_2 particles were easily reunited because of the surface effect, which suppressed the crystallization and growth of the $Ti_2Al_{20}Ce$ crystal.

Stepanova *et al* (2000) reported that usually TiCN is added to the melt as a tablet sintered with a metal-activator, changing the addition interaction with the liquid alloy. As mentioned above, Ce was able to prevent growth of the $TiC_{0.3}N_{0.7}$ crystal. Thus, $TiC_{0.3}N_{0.7}$ exhibited a fine microstructure (see figure 4d). The production of the carbonitrides provided hardening and wear resistance of the composite coating. An earlier study revealed that nano-CeO_2 prevented the coatings from defects and improved the quality of the coatings surface (Shen *et al* 1997). Grain boundary was also purified by cerium concentration. Thus, the crack tendency of the coatings decreased. Furthermore, it should be considered that during the laser cladding process, CeO_2 absorbed amount of energy from the laser beam, which can decrease the existing time of the molten pool and also accelerate the super-cooling degree. Thus, the diffusibility of the particles in this molten pool was prevented to a certain extent.

3.3 *Microhardness distributions and wear resistance*

The microhardness as a function of depth from the coating surface to the Ti–6Al–4V substrate is shown in figure 5. It can be seen that the microhardness of coating in sample 1 was in the range of $1100 \sim 1250$ $HV_{0.2}$ due to the action of the Ti_3Al+TiC/TiN+$TiC_{0.3}N_{0.7}$ hard phases. Furthermore, it was noted that the microhardness of the coating in sample 2 was in the range of $1200 \sim 1350$ $HV_{0.2}$, which was higher than that of sample 1 due to the massive dilution of the TiC/TiN primary particles.

It was also noticed that with the addition of nano-CeO_2, microhardness of the coating in sample 3 was higher than that of sample 2 (see figure 6). The enhancement of microhardness of the coating in sample 3 can be ascribed to the actions of the $Ce(CN)_3$, CeO_2, $Ti_2Al_{20}Ce$ phases and fine grain strengthening.

When the load was 5 kg, wear test result revealed that the wear volume loss of the substrate was ∼2 times higher than

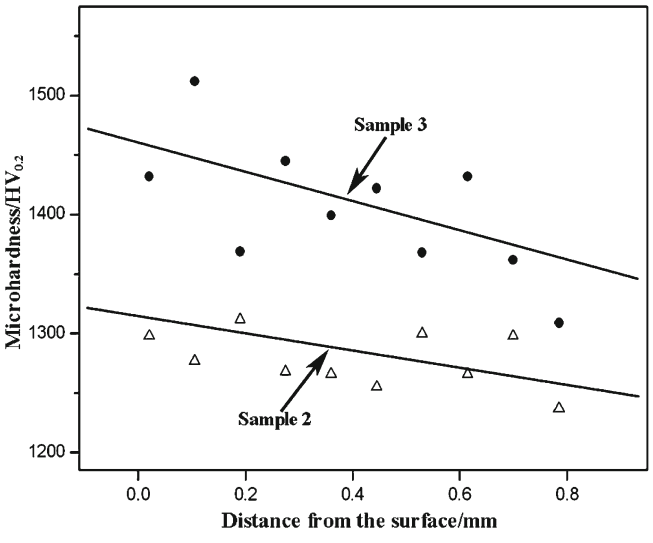

Figure 6. Microhardness distributions of coatings in samples 2 and 3.

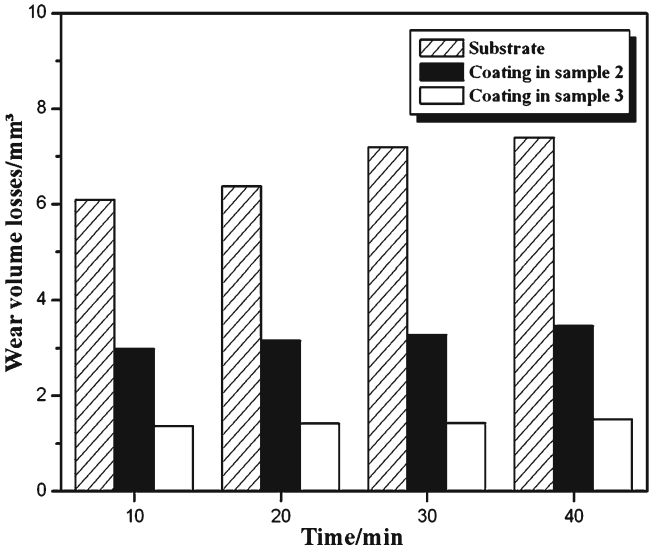

Figure 7. Wear mass losses of composite coatings in samples 2, 3 and Ti–6Al–4V alloy.

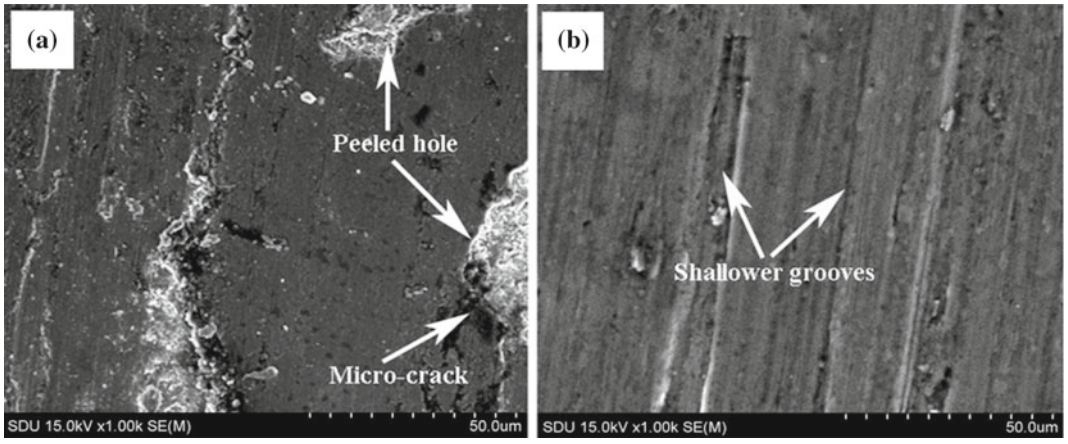

Figure 8. Worn morphologies of (**a**) coating surface in sample 2 and (**b**) coating surface in sample 3.

that of the coating in sample 2. However, wear volume loss of the coating in sample 3 was ~4·5–5 times less than that of the substrate (see figure 7). It was considered that due to higher microhardness, the coating in sample 3 exhibited better wear resistance than that of the coating in sample 2. Moreover, it should be mentioned that the coating in sample 1 showed poor wear resistance mainly due to its poor quality of the microstructure.

SEM micrographs showed that when the load was 5 kg, deep peeled holes and micro-crack were produced in the coating surface of sample 2 (see figure 8). Nevertheless, the coating surface in sample 3 showed shallow grooves free of dip, hole and micro-crack. As mentioned previously, Ce was able to improve strength and ductility of the coatings. Thus, under action of wear plate, the dip peeled hole and micro-crack were not present in the coating surface of sample 3.

4. Conclusions

Laser cladding of the Al_3Ti+TiC/TiN pre-placed powders on the Ti–6Al–4V alloy can form the TiC/TiN+TiCN reinforced composite coating, which improved wear resistance of the Ti–6Al–4V alloy. There were Ti_3Al or Ti_3Al/Al_3Ti, TiC, TiN and $TiC_{0.3}N_{0.7}$ in the Al_3Ti+TiC/TiN laser-cladded coating. Nano-CeO_2 can suppress crystallization and growth of the precipitates to a certain extent, thus resulting in fine microstructure. With the addition of proper content of nano-CeO_2, the microhardness and wear reistance of the Al_3Ti+TiC/TiN laser-cladded coating were significantly improved due to the actions of the $Ce(CN)_3/CeO_2/Ti_2Al_{20}Ce$ phases and high quality microstructure. The wear volume loss of the Al_3Ti+TiC/TiN+nano-CeO_2 laser-cladded coating was ~4·5–5 times less than that of the Ti–6Al–4V alloy.

Acknowledgements

This work was supported by the Development Project of Science and Technology of Shandong Province (2010GGX10403).

References

Baligidad R G and Khaple S 2009 *Bull. Mater. Sci.* **32** 531
Dutta Majumdar J, Mordike B L and Manna I 2000 *Wear* **242** 18
Dutta Majumdar J, Manna I, Kumar A, Bhargava P and Nath A K 2009 *J. Mater. Process. Technol.* **209** 2237
Ertuerk E, Knotek O, Bergmer W and Prengel H-G 1991 *Surf. Coat. Technol.* **46** 39
Forn A, Picas J A, Fuentes G G and Elizalde E 2001 *Int. J. Refract. Met. Hard Mater.* **19** 507
Hisashi S, Takashi M, Toshiyuki F, Susumu O, Yoshimi W and Masaharu K 2008 *Acta Mater.* **56** 4549
Lai F D, Wu T I and Wu J K 1993 *Surf. Coat. Technol.* **58** 79
Li M X, Zhang S H, Li H S, He Y Z, Yoon J H and Cho T Y 2008 *J. Mater. Process. Technol.* **202** 107
Shen Y F, Chen J Z, Feng Z C and Liang Y 1997 *J. Chinese Rare Earth Soc.* **15** 344
Stepanova N N, Rodionov D P, Sazonova V A and Khlystov E N 2000 *Mater. Sci. Eng.* **A284** 88
Tian Y S, Chen C Z, Chen L X and Huo Q H 2006 *Scr. Mater.* **54** 847
Wang J, Li Y J and Gerasimov S A 2007 *Bull. Mater. Sci.* **30** 415
Wang X H, Zhang M and Qu S Y 2010 *Opt. Laser Technol.* **48** 893
Yang Y L, Yao W M and Zhang H Z 2010 *Surf. Coat. Technol.* **205** 620
Zeng Y, Lee S W, Gao L and Ding C X 2002 *J. Eur. Ceram. Soc.* **22** 347
Zhang S H, Li M X, Cho T Y, Yoon J H, Lee C G and He Y Z 2008 *Opt. Laser Technol.* **40** 716
Zhao T, Xun C, Wang S X and Zheng S A 2000 *Thin Solid Films* **379** 128
Zhao H L, Song Y, Li M and Guan S K 2010 *J. Alloy Compd.* **508** 206